THE JOURNAL OF BIOLOGICAL CHEMISTRY
Vol. 278, No. 45, Issue of November 7, pp. 44929–44934, 2003
Printed in U.S.A.

Differential Regulation of Exocytotic Fusion and Granule-Granule Fusion in Eosinophils by Ca^{2+} and GTP Analogs*

Received for publication, June 9, 2003, and in revised form, June 30, 2003
Published, JBC Papers in Press, July 9, 2003, DOI 10.1074/jbc.M306014200

Jana Hartmann‡, Susanne Scepek§, Ismail Hafez§, and Manfred Lindau§¶

From the ‡Institut für Physiologie, Ludwig-Maximilians-Universität München, Pettenkoferstrasse 12, D-80336 München, Germany and the §School of Applied and Engineering Physics, Cornell University, Ithaca, New York 14853

Dynamics of degranulation was studied in horse eosinophils by patch clamp capacitance measurements. Degranulation was stimulated by intracellular application of calcium, and GTPγS or guanosine 5′-(β,γ-imido)-triphosphate at different concentrations via the patch pipette. Degranulation was quantified by measuring the delay time between the beginning of intracellular perfusion and the first exocytotic event, determining the distribution of time intervals between fusion events and the capacitance step size distributions under the different conditions. The degranulation dynamics could be well reproduced using a computer model assuming three independent rate constants for granule-plasma membrane fusion, granule fusion with already exocytosed granules, and intracellular granule-granule fusion. The rate of granule-plasma membrane fusion is sensitive to both, the GTP analog and $[Ca^{2+}]_i$. The rate of granule-exocytosed granule fusion is sensitive to $[Ca^{2+}]_i$ but insensitive to the GTP analogs, and the rate of granule-to-granule fusion is sensitive to the GTP analog but insensitive to $[Ca^{2+}]_i$. Granule fusions with the three different target compartments thus involve different regulatory mechanisms.

In many cell types release of preformed materials stored in secretory vesicles or granules occurs by the mechanism of exocytosis, *i.e.* by fusion of the perigranular membrane with the plasma membrane. Eosinophils play an important role in killing of multicellular parasites (1). After contact with the parasite surface the cytotoxic proteins stored within the secretory granules are released onto the parasite surface. Following adherence the appearance of large cytoplasmic vacuoles was thought to reflect multigranular compounds formed by granule-granule fusion directing the contents of many granules to a single release site (2–5). Using simultaneous fluorescence imaging and whole-cell membrane capacitance measurements and electron microscopy we have shown that in eosinophils focal release of granular contents is achieved by intracellular granule-granule fusion followed by compound exocytosis and also by cumulative fusion of granules with the membrane of a granule that had already fused with the plasma membrane (35).

A number of experiments indicate that in addition to their capability to fuse with the plasma membrane, secretory granules are also able to perform homotypic fusion among themselves. High intracellular calcium ($[Ca^{2+}]_i$) stimulates fusion among cortical granules from sea urchin eggs (6), and fusion among chromaffin granules was obtained in the presence of high calcium, annexins, and arachidonic acid (7). Fusion among dense core vesicles was observed in pituitary nerve terminals in the presence of 50–100 μM $[Ca^{2+}]_i$ (8), and extensive fusion among secretory granules was stimulated by intracellular application of 80–160 μM GTPγS in eosinophils (9, 10). Granule-granule fusion has recently been directly imaged in pituitary lactotrophs (11, 12), and patch clamp and amperometric techniques provided evidence for compound exocytosis in neutrophils (13) and β-cells (14). Evidence for cumulative fusion of granules with the membrane of previously exocytosed granules has been found in eosinophils (10, 35) as well as pituitary lactotrophs (12) and pancreatic acinar cells (15).

Here we demonstrate that the three different types of fusion events occurring during eosinophil degranulation, namely granule-plasma membrane fusion, and granule-granule fusion and granule-fused granule fusion, are differentially controlled by intracellular second messengers and that granule-granule fusion is selectively stimulated by extracellular stimulation with concanavalin A (ConA).[1]

EXPERIMENTAL PROCEDURES

Cell Preparation—Horse eosinophils were isolated from fresh blood from the jugular vein of horses and purified over discontinuous Percoll gradients as described (10). Isolated cells were suspended in Medium 199 containing 4 mM glutamine, 4.2 mM $NaHCO_3$, and penicillin/streptomycin, pH 7.3–7.4, stored at room temperature, and used within 2–4 days.

Patch Clamp Experiments—About 50–100 μl of the cell suspension were transferred into a Petri dish with a coverslip as bottom. After a few minutes to allow the cells to settle on the glass, the dish was perfused with standard external saline (140 mM NaCl, 5 mM KCl, 2 $CaCl_2$, 1 mM $MgCl_2$, 10–20 mM glucose, 10 mM HEPES/NaOH, pH 7.2–7.3). The whole-cell configuration with the contact between the cytosol and the solution inside the micropipette was used to internally perfuse the cells. The internal solution contained 125 mM potassium-L-glutamate, 10 mM NaCl, 7 mM $MgCl_2$, 1 mM Na_2ATP, and 10 mM HEPES/NaOH, pH 7.2–7.3. $CaCl_2$, EGTA, GTPγS, and guanosine 5′-(β,γ-imido)triphosphate (Gpp(NH)p) were varied as follows. For experiments at high intracellular calcium concentration ($[Ca^{2+}]_i$), the pipette solutions contained 5 mM EGTA and 4.5 mM $CaCl_2$, the resulting $[Ca^{2+}]_i$ was calculated to be 1.5 μM. In the solutions with low $[Ca^{2+}]_i$ (<10 nM) 7 mM EGTA was added and $CaCl_2$ was omitted. The osmolarity of the external solution was adjusted with D(+)glucose until it exceeded the internal solution by a few mosmol. All experiments were done at room temperature.

Capacitance Measurements—The change of cell membrane capacitance was measured as the imaginary component of the admittance change of the cell using a lock-in amplifier and a EPC-9 patch clamp

* This work was supported by National Institutes of Health Grant R01 NS38200 (to M. L.). The costs of publication of this article were defrayed in part by the payment of page charges. This article must therefore be hereby marked "*advertisement*" in accordance with 18 U.S.C. Section 1734 solely to indicate this fact.

¶ To whom correspondence should be addressed: School of Applied and Engineering Physics, Cornell University, Ithaca, NY 14853. Tel.: 607-255-5264; Fax: 607-255-7658; E-mail: ml95@cornell.edu.

[1] The abbreviations used are: ConA, concanavalin A; Gpp(NH)p, guanosine 5′-(β,γ-imido)triphosphate; t-SNARE, target soluble NSF attachment protein receptors.

amplifier (List Electronics, Darmstadt, Germany). Command voltage signal was an 800 Hz, 20 mV (root mean square) sine wave, and the current output signal was analyzed by a 2-phase lock-in amplifier (5210, EG&G PAR, Princeton, NJ) (16) and sampled by the computer every 22 ms. After attaining the whole-cell configuration the bulk capacitance of the cell was compensated. During the measurement of the capacitance the phase error of the lock-in was determined using the phase tracking technique (17).

Quantification of Capacitance Changes—The delay, time intervals, and step size ΔC_m of a distinct capacitance increase in consequence of a fusion of a granule with the plasma membrane were determined by visual examination of the capacitance traces on the computer screen using cursor lines (Fig. 1). To calculate the percentage of capacitance increase generated by steps in a certain range (bin), the number of steps in that bin was multiplied with the step size corresponding to the center of the bin and divided by the total capacitance increase generated by the sum of all steps in the distribution.

Computer Simulation of Degranulation—Computer simulations were performed assuming resting cells with 50 granules, each of them formed by the fusion of 1 to 21 unit granules with a capacitance of 6 fF. The size of the granules, expressed in numbers of fused unit granules, was normally distributed with a maximum at 11 unit granules, similar to the distribution observed experimentally (18). The model uses three different rate constants for granule-plasma membrane fusion (k_{gp}), granule-exocytosed granule fusion (k_{ge}), and intracellular granule-granule fusion (k_{gg}). The individual probability for the fusion of a particular single granule was assumed to be proportional to its membrane area. The granules were polled 6000 times in 150 ms intervals to determine whether a fusion event occurred during this time interval. For each cell the degranulation is therefore simulated for a duration of 15 min. The simulation yields a capacitance trace with steps according to the size of the fused granules and separated by the corresponding time intervals analogous to experimental recordings but free of noise. In addition, the computer program tracks the number of degranulation sacs for each cell. For each set of parameters, k_{gp}, k_{ge}, and k_{gg}, 30 simulations were carried out and the simulated capacitance traces were analyzed to determine delay, time intervals between steps, and step sizes, exactly like the experimental recordings.

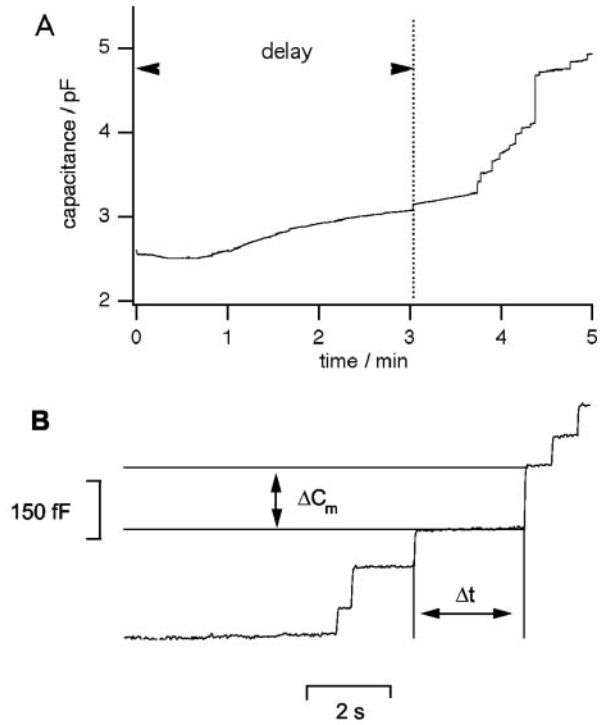

FIG. 1. **Quantitative analysis of a capacitance trace measured during the degranulation of a horse eosinophil.** The delay is the time between beginning of intracellular perfusion with the pipette solution and the first capacitance step (*A*). The individual capacitance step sizes ΔC_m and the time intervals between successive steps Δt were measured with cursor lines on the computer screen (*B*).

RESULTS

High $[Ca^{2+}]_i$ Facilitates Exocytotic Fusion, but Not Granule-to-Granule Fusion—In mast cells (19), neutrophils (20), and eosinophils (21) intracellular application of GTPγS stimulates degranulation. The kinetics of exocytosis is modulated by the intracellular free calcium concentration $[Ca^{2+}]_i$ (20, 22, 23). To test whether both exocytosis and granule-granule fusion in eosinophils are influenced by $[Ca^{2+}]_i$ in the same way, cells were internally dialyzed with pipette solutions containing either 7 mM EGTA ($[Ca^{2+}]_i < 10$ nM) or 5 mM EGTA and 4.5 mM $CaCl_2$ ($[Ca^{2+}]_i \sim 1.5$ μM) in the presence of GTPγS. To characterize the dynamics of degranulation three parameters were analyzed: i) the delay between patch rupture and the first capacitance step (Fig. 1*A*), indicating the time between beginning of internal dialysis and the first fusion of a specific granule with the plasma membrane; ii) the time intervals between consecutive capacitance steps indicating the time intervals between exocytotic fusion events (Fig. 1*B*); and iii) the capacitance step size distributions indicating the extent of granule-granule fusion preceding exocytosis of granules or multigranular compounds (Fig. 1*B*).

The mean delays obtained under the different experimental conditions are shown in Fig. 2*A* as the *shaded bars*. At a given GTPγS concentration the delay is about 3-fold longer at low $[Ca^{2+}]_i$ than at high $[Ca^{2+}]_i$. The prolongation is 3.1-fold with 20 μM and 2.6-fold with 80 μM GTPγS. The delay also tends to be shorter at the higher GTPγS concentration. Even when the stimulation conditions are kept constant, the delay observed in individual degranulations varied substantially from one cell to another. We formally calculated the standard deviations to quantify the scatter (Fig. 2*B*, *solid lines*), although the distributions of delays were not gaussian.

The frequency distributions of the time intervals between two subsequent fusion events obtained for the different experimental conditions are shown in Fig. 3*A*. The distributions decay exponentially, and the corresponding rates of exocytosis were determined by single exponential fits. The time constants at high $[Ca^{2+}]_i$ were 4.8 s (exocytotic rate $k = 0.21\ s^{-1}$ at 20 μM GTPγS) and 4.5 s ($k = 0.22\ s^{-1}$ at 80 μM GTPγS). At low $[Ca^{2+}]_i$ the time constant was 11.1 s at both GTPγS concentrations (exocytotic rate $k = 0.09\ s^{-1}$ at 20 and 80 μM GTPγS). The exocytotic rate during degranulation is thus independent of the GTPγS concentration but at $[Ca^{2+}]_i \sim 1.5$ μM the rate of exocytotic fusion events is ~2.4-fold higher compared with that at $[Ca^{2+}]_i < 10$ nM.

As in other secretory systems (24), and as for transducin (25) and G_S (26), another poorly hydrolyzable GTP-analog, Gpp(NH)p, is expected to be also stimulatory but with lower potency. When cells were internally dialyzed with a solution containing Gpp(NH)p complete degranulation was induced as well. However, compared with GTPγS about 10 times higher concentrations of Gpp(NH)p were required to attain similar delays, rates of exocytotic events, and step size distributions (data not shown).

Besides exocytotic fusion, GTPγS at high concentrations stimulates intracellular granule-granule fusion as indicated by the occurrence of very large capacitance steps (10) and as demonstrated directly by fluorescence imaging and electron microscopy (35). The number and size of large steps depends on the ratio of the rates at which granule-to-granule fusion and exocytotic fusion occur (9). If $[Ca^{2+}]_i$ had a similar effect on both rates, then the step size distributions should not be affected by $[Ca^{2+}]_i$. However, if $[Ca^{2+}]_i$ accelerates only the exocytotic rate and has no effect on the rate of intracellular granule-granule fusion, then the steps should become larger at low $[Ca^{2+}]_i$ because more time would remain for the granules to fuse with each other before the compounds fuse with the

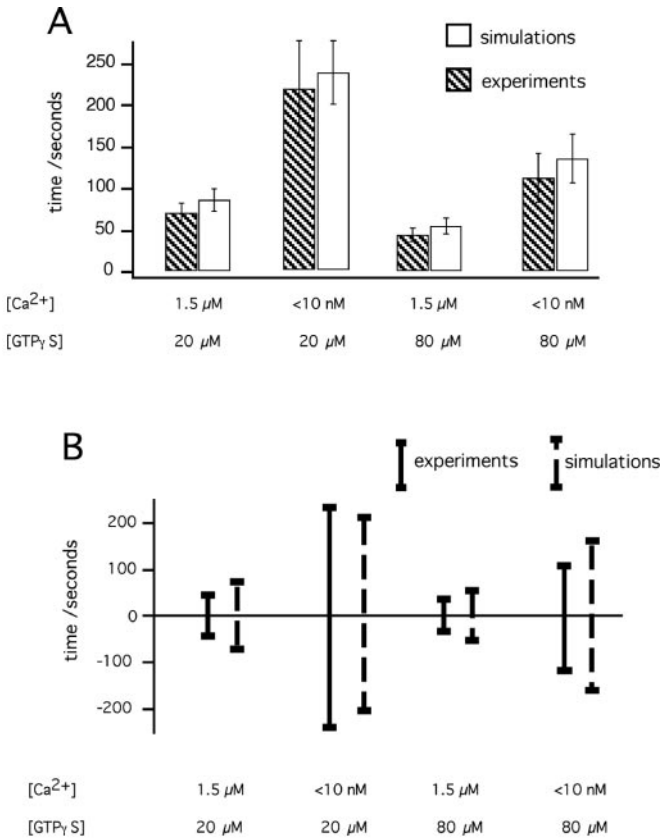

FIG. 2. **Mean delays ± S.E. (*A*) and standard deviations (*B*) between the beginning of intracellular dialysis with the pipette solution and the first exocytotic fusion event under different experimental conditions.** *Shaded bars* are for experimental data, *open bars* for simulated data (parameters are given in Table I).

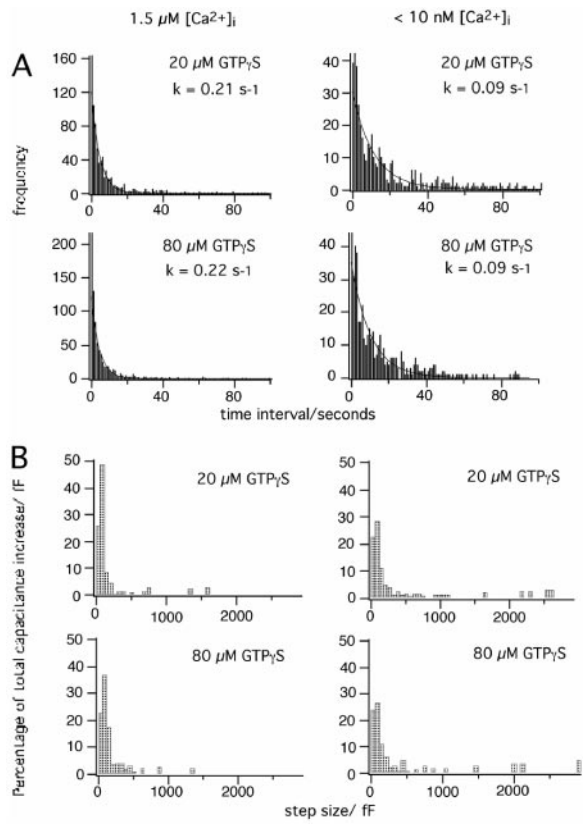

FIG. 3. **Statistical analysis of degranulation dynamics.** *A*, frequency distributions of the time intervals between adjacent capacitance steps for different concentrations of GTPγS and free Ca^{2+} (*vertical lines*). The distributions were fitted by single exponentials (*smooth decaying lines*) giving the indicated rate constants (k). *B*, capacitance step size distributions obtained under the different experimental conditions.

plasma membrane. Indeed the number of steps <200 fF decreases and more large steps occur in experiments with low $[Ca^{2+}]_i$ (Fig. 3*B*).

Simulation of the Degranulation—To determine whether the change in step sizes is quantitatively explained by a $[Ca^{2+}]_i$ dependence of the exocytotic rate alone, degranulation was simulated using a model with three distinct rate constants for three different fusion processes (9) (Fig. 4*A*). In this model we allow a granule to fuse either directly with the plasma membrane (rate k_{gp}), with another granule (rate k_{gg}), or with the membrane of an already exocytosed granule (rate k_{ge}). All three rate constants are defined per unit area of membrane such that the probabilities for fusion are proportional to the surface areas of the fusing compartments. Using combined fluorescence imaging and equivalent circuit analysis we have shown that during degranulation of eosinophils a degranulation sac is formed by cumulative fusion events (35). Granule-plasma membrane fusion is thus a rare event during eosinophil degranulation, and the rate of exocytotic events during degranulation is thus dominated by the rate of granule-exocytosed granule fusion k_{ge}. The delay exclusively depends on the rate k_{gp} because the target compartment for granule-exocytosed granule fusion does not exist before the first exocytotic event occurs. Accordingly, the value of k_{gp} was estimated from the experimentally observed delays. The rate constant k_{ge} for fusion of a granule with already exocytosed granules was deduced from the exocytotic rate that depends on $[Ca^{2+}]_i$. The resulting step size distribution essentially depends only on the ratio of k_{gg} *versus* the exocytotic rates k_{ge} and k_{gp}.

Examples of simulated traces for two different sets of rate constants are shown in Fig. 4*B*. Due to the stochastic simulation method, each simulated trace was different even when the same set of rate constants was used, just as in experiments where the exact time course of degranulation of one cell is never repeated by a second cell. The simulated traces were statistically analyzed in the same way as the experimentally measured traces. Using the rate constants given in Table I good correspondence between simulated degranulations and the experimental results was obtained for the four different experimental conditions.

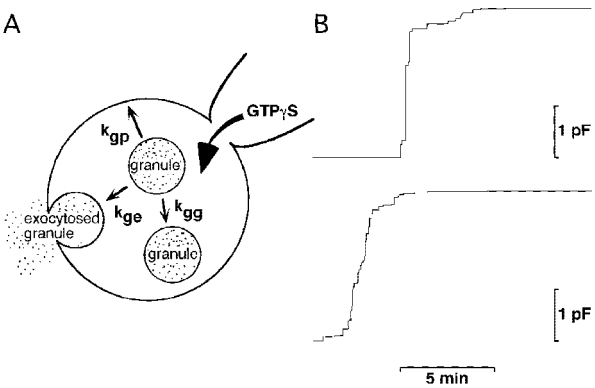

FIG. 4. *A*, degranulation model with three different fusion processes and the corresponding rate constants. The fusion probabilities are assumed to be proportional to the membrane areas of the two fusing membranes. *B*, representative simulated capacitance traces obtained with two different sets of rate constants as given in Table I. *Upper trace*, low $[Ca^{2+}]_i$, 20 μM GTPγS; *lower trace*, high $[Ca^{2+}]_i$, 80 μM GTPγS.

The mean values of the delays occurring in the simulations

TABLE I
Parameters used to simulate the degranulations

All rate constants are given in $s^{-1}\ \mu m^{-4}$. For each of the four parameter sets 30 degranulations were simulated and analyzed in the same way as the experimental recordings.

$[Ca^{2+}]_i$	GTPγS	k_{gp}	k_{ge}	k_{gg}
<10 nM	20 μM	3.2×10^{-8}	4.6×10^{-6}	1.1×10^{-6}
1.5 μM	20 μM	8.2×10^{-8}	1.2×10^{-5}	1.1×10^{-6}
<10 nM	80 μM	5.6×10^{-8}	4.6×10^{-6}	1.8×10^{-6}
1.5 μM	80 μM	1.5×10^{-7}	1.2×10^{-5}	1.8×10^{-6}

are shown in Fig. 2*A* as the *unshaded bars*. The data are in very good agreement with those obtained from experimental recordings. In addition, also the standard deviations of the delays obtained in the simulations (Fig. 2*B*, *dashed lines*) are similar to the experimentally observed standard deviations (*solid lines*). The frequency distributions of the time intervals between successive capacitance steps in the simulations are shown in Fig. 5*A*. As for the experimental data, the distributions are well fitted by single exponentials, and the fits gave the same apparent rates as those obtained experimentally (Fig. 3*A*). Fig. 5*B* shows the step size distributions obtained in the simulations. As in the experiments, the number of small steps decreases and additional large steps occur in simulations using parameters for low $[Ca^{2+}]_i$. The simulations provide an interesting result. The rate k_{gg} depends only on the GTPγS concentration, k_{ge} depends only on $[Ca^{2+}]_i$, and k_{gp} depends on both $[Ca^{2+}]_i$ and GTPγS concentration (Table I).

Concanavalin A Stimulates Granule-to-Granule Fusion—Using electron microscopy it was observed that the lectin ConA induces the emergence of large vacuoles inside eosinophils (27). To test if this observation reflects stimulation of granule-to-granule fusion in intact cells, we performed capacitance measurements on cells preincubated with ConA.

Cells incubated with 20 μg/ml ConA for one hour had an initial capacitance $C_i = 3.1 \pm 0.4$ pF (S.D., $n = 19$), indistinguishable from that of control cells with $C_i = 3.0 \pm 0.4$ (S.D., $n = 27$). Thus, the plasma membrane area had not increased during incubation. When the cells were internally dialyzed with a solution containing 5 μM GTPγS ($[Ca^{2+}]_i \sim 1.5$ μM), the cell capacitance increased by 3.9 ± 0.9 pF (S.D., $n = 18$), not significantly different from control cells not incubated with ConA (4.0 ± 0.9, S.D., $n = 27$). These results indicate, that ConA did not stimulate degranulation during the one hour incubation because plasma membrane area did not increase, and the same amount of granules is present inside the cells after incubation with ConA and can be stimulated to be exocytosed by GTPγS.

Fig. 6*A* shows the effect of the ConA incubation on the step size distribution. After incubation with ConA many large steps of up to 700 fF capacitance occur in the presence of only 5 μM GTPγS, whereas at this GTPγS concentration no steps >300 fF were seen in control cells (Fig. 6*A*). The exocytotic rates determined from the frequency distributions of time intervals between exocytotic events (Fig. 6*B*) were similar in ConA-treated cells and control cells. These results indicate that ConA does not stimulate exocytosis, but stimulates intracellular granule-granule fusion. The thus formed multigranular compounds then fuse with the plasma membrane, when exocytosis is stimulated by intracellular GTPγS.

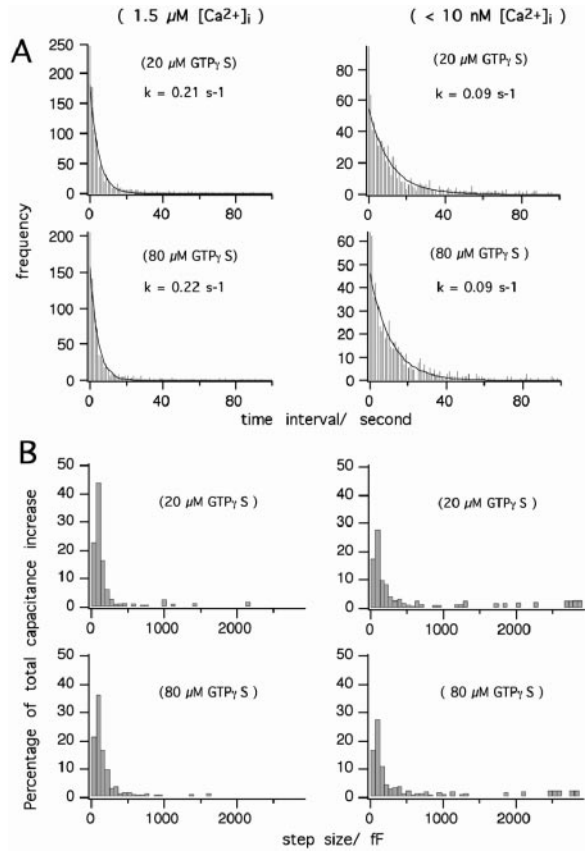

FIG. 5. **Statistical analysis of simulated degranulation traces.** The rate constants used to simulate the degranulation dynamics under the different experimental conditions, as indicated in *parentheses*, are listed in Table I. *A*, frequency distributions of the time intervals between capacitance steps. *B*, step size distributions determined from simulated degranulation traces.

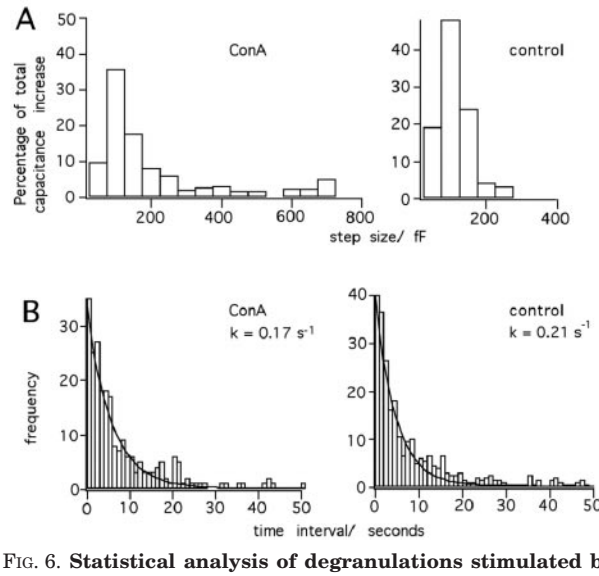

FIG. 6. **Statistical analysis of degranulations stimulated by 5 μM intracellular GTPγS in cells preincubated with 20 μg/ml ConA for 1 h (*left panels*) and control cells (*right panels*).** *A*, step size distributions. *B*, frequency distributions of time intervals. The rate constants were obtained by single exponential fits.

DISCUSSION

In eosinophils three different fusion processes of secretory granules have been identified (35): exocytotic fusion of secretory granules with the plasma membrane, cumulative fusion of granules with the membrane of already exocytosed granules, and intracellular fusion among cytoplasmic granules. The dynamics of degranulation can be well reproduced using a simple model assuming three distinct rate constants for the fusion events with the three different target membranes. We have shown here that the different rate constants are differently affected by $[Ca^{2+}]_i$ or the type or concentration of the poorly

hydrolyzable GTP analog used.

Uniqueness of the Model—The first important question to be asked is if the set of parameters given in Table I is unique or if other values for the different rates under certain experimental conditions would reproduce the data as well. The first parameter is the rate for granule-plasma membrane fusion k_{gp}. This rate alone determines the delay. For a given total area of granule membrane and plasma membrane, which does not vary much among cells, the rates k_{gp} that provide delays in the simulation that agree with the experimentally observed delays are unique. The delays that come from the model are completely independent of the choices for k_{ge} and k_{gg}. The independence of k_{ge} is obvious because the target compartment does not exist before the first fusion event occurs. The reason for the independence of k_{gg} is that the fusion probability for a granule or compound is assumed to be proportional to its total membrane area. Thus, the probability for the first fusion event to occur is the same when all granules are still individual ones or when some or even all of them have fused into a large compound.

The rates at which exocytotic events occur, once the first granule or compound was exocytosed, is dominated by the rate k_{ge}. Combined fluorescence imaging and admittance analysis have shown that once exocytosis has occurred, granules preferentially fuse with previously exocytosed granules leading to an enlarging degranulation sac (10, 35). The experimentally observed independence of the rate at which exocytotic events occur following the delay of the GTPγS concentration requires that the rate k_{ge} that dominates this parameter is independent of the GTPγS concentration. Again, the exocytotic rate is independent of the degree of granule-granule fusion because the fusion rate of a compound or granule is expected to be proportional to its membrane area. Once these rates are determined, the rate k_{gg} must then be varied such that the observed capacitance step size distributions that are measured under certain experimental conditions are reproduced. This variation must be done without varying k_{gp} and k_{ge} because any variations of these would change the delay or the rate of exocytotic events and these changes cannot be compensated by changes of k_{gg}. The sets of parameters for the rates k_{gp}, k_{gg}, and k_{ge} are thus unique. The only assumption made in the model is that the fusion probability of a granule or compound is proportional to its membrane area. We consider this the most likely possibility because the number of potential fusion sites or fusion machines should be directly proportional to the membrane area.

Ca^{2+} Regulates Granule-Plasma Membrane Fusion and Granule-exocytosed Granule Fusion—$[Ca^{2+}]_i$ affects the delay and the time intervals between exocytotic fusion events. This observation fits well with previous results obtained for mast cells and neutrophils where degranulation can also be stimulated by intracellular application of poorly hydrolyzable GTP-analogs, even when $[Ca^{2+}]_i$ is buffered below resting levels (20, 22, 28). In mast cells the exocytotic rate increases during transient elevations of $[Ca^{2+}]_i$ (22) and in neutrophils the delay becomes longer and the exocytotic rate decreases when $[Ca^{2+}]_i$ is buffered below resting levels (23). In contrast to the exocytotic rates k_{gp} and k_{ge}, the rate of intracellular granule-granule fusion k_{gg} is not significantly affected by $[Ca^{2+}]_i$ but is strongly dependent on the type and concentration of the GTP analog used. This result is in line with a report showing that in macrophages intracellular granule-phagosome fusion is a calcium-independent event (29).

Upon Exocytosis the Granule Membranes Become Highly Fusogenic—Following the first exocytotic events, granules fuse preferentially with the membrane of already exocytosed granules. In our model, the marked transition in fusion competence, which occurs in the granule membrane upon its exocytosis, is assumed to be instantaneous. Thus, a rapid change must occur, the nature of which remains to be elucidated. Upon exocytotic fusion the granular membrane potential is rapidly discharged and the intragranular milieu changes its pH and composition. This may lead to a change in membrane tension but could also result in specific changes in transmembrane proteins that might be involved in the fusion process. Evidence for cumulative fusion of granules with granules already fused with the plasma membrane has recently been obtained in pituitary lactotrophs (12), the ribbon synapse (30), and pancreatic acini (15). It was suggested that cumulative granule-fused granule fusion may be dependent on a diffusible factor in the membrane (possibly a t-SNARE) that moves from the plasma membrane to the first fused granule and subsequently into the membrane of other granules fused with the exocytotic structure making the membranes fusion competent (15). However, in eosinophils intracellular homotypic granule-granule fusion does occur indicating that the granules contain functional t-SNAREs and diffusion of a t-SNARE from the plasma membrane into membranes of exocytosed granules may not be required. In fact, granule plasma membrane fusion is a rare event in eosinophils suggesting that the enhanced fusion competence of the membranes of exocytosed granules is not based on t-SNARE diffusion from the plasma membrane.

GTPγS Modulates Granule-Plasma Membrane Fusion but Not Granule-exocytosed Granule Fusion—We found that in eosinophils the rate of granule-exocytosed granule fusion is completely insensitive to the type and concentration of GTP analogs. It may be possible that granule fusion with exocytosed granules would even occur in the absence of any poorly hydrolyzable GTP analog, but this possibility could not be tested because in the absence of GTPγS or Gpp(NH)p the target compartment does not exist. If activation of granule-exocytosed granule fusion also involves GTP binding proteins, then these must have much higher sensitivity to the GTP analogs and must thus be different from those GTP binding proteins mediating the rates k_{gp} and k_{gg}.

In pituitary lactotrophs, growing exocytotic sites were observed by fluorescence imaging, suggesting that this mechanism may actually involve cumulative fusion (12). Forskolin, which increases intracellular cAMP, was found to stimulate compound exocytosis whereas granule-plasma membrane fusion was unchanged (12). This data also points to a differential regulation of granule-plasma membrane fusion and granule-exocytosed granule fusion.

Evidence for compound exocytosis and in particular cumulative fusion has come from studies on pancreatic acinar cells (15), pituitary lactotrophs (12), and the ribbon synapse (30). In all these cell types secretion is directed toward a certain site that is pre-defined by the tissue morphology, and it appears that a mechanism of cumulative fusion effectively targets granular contents to focal sites. In eosinophils focal release is also an important feature of exocytosis for effective parasite killing. In contrast to tissue cells, however, the site of release is not pre-defined in circulating granulocytes but is defined by the stimulus, the contact with the parasite surface. Cumulative fusion thus appears to be a widely conserved mechanism of focal release from several granules in a wide variety of cell types.

Intracellular Granule-Granule Fusion Is Modulated by GTP Analogs but Not by Ca^{2+}—There is clear evidence for homotypic granule-granule fusion and compound exocytosis for several granule types including chromaffin granules (7), sea urchin egg cortical granules (6), dense core vesicles in pituitary nerve terminals $[Ca^{2+}]_i$ (8), eosinophils (10, 31), neutrophils

(13), lamellar bodies of alveolar type II cells (32), pancreatic β-cells (14), granules of pituitary lactotrophs (11, 12), and pancreatic acinar cell zymogen granules (33). In eosinophils, the rate of granule-granule fusion is not affected by $[Ca^{2+}]_i$ but is strongly dependent on the type and concentration of the GTP analog used. It is possible that relocation of SNAP-23 (soluble NSF attachment protein of 23 kD molecular weight) from the cell surface to granule membranes is involved in this mechanism (34). Homotypic zymogen granule-granule fusion also was found to have a markedly lower Ca^{2+} sensitivity than zymogen granule-plasma membrane fusion (33). We found no $[Ca^{2+}]_i$ dependence of granule-granule fusion between 10 nM and 1.5 μM in eosinophils. Due to the $[Ca^{2+}]_i$ dependence of the exocytotic fusion rates compound exocytosis is actually less prominent at 1.5 μM than at 10 nM $[Ca^{2+}]_i$. The pronounced effects of GTP analogs on granule-granule fusion suggest that the main regulatory mechanisms for granule-granule fusion differs from that of exocytotic fusion. The regulation of granule-granule fusion by GTP-binding proteins may be specific for granulocytes as granule-granule fusion seemed unaffected by GTPγS in alveolar type II cells (32).

What is the functional significance of homotypic fusion among secretory granules in eosinophils? We have shown here that stimulation of intact cells with the lectin ConA induces granule-to-granule fusion without activating exocytosis. ConA presumably exerts its effect via receptor cross-linking in the plasma membrane. The selective activation of granule-granule fusion by a cross-linker suggests that the extent of cross-linking may be the mechanism controlling the degranulation mode. Following adherence of the cell to a large parasite surface, discharge of all granular contents at the attachment site is desirable and massive granule-to-granule fusion followed by exocytosis of the compound would be most efficient to perform this task. In eosinophils homotypic granule-granule fusion thus appears to be an essential cellular process, which may be important in targeting the contents of many secretory granule to a single release site (10). Differential regulation of the different types of fusion events as described here are essential to modulate the degranulation mode depending on the type of stimulus.

REFERENCES

1. Butterworth, A. E. (1977) *Curr. Top. Microbiol. Immunol.* **77,** 127–168
2. McLaren, D. J., Mackenzie, C. D., and Ramalho-Pinto, J. F. (1977) *Clin. Exp. Immunol.* **30,** 105–118
3. McLaren, D. J., Ramalho-Pinto, F. J., and Smithers, S. R. (1978) *Parasitology* **77,** 313–324
4. Glauert, A. M., Butterworth, A. E., Sturrock, R. F., and Houba, V. (1978) *J. Cell Sci.* **34,** 173–192
5. Scepek, S., Moqbel, R., and Lindau, M. (1994) *Parasitol. Today* **10,** 276–278
6. Vogel, S. S., and Zimmerberg, J. (1992) *Proc. Natl. Acad. Sci. U. S. A.* **89,** 4749–4753
7. Drust, D., and Creutz, C. E. (1988) *Nature* **331,** 88–91
8. Lindau, M., Rosenboom, H., and Nordmann, J. J. (1994) in *Molecular and Cellular Mechansisms of Neurotransmitter Release* (Stjärne, L., Greengard, P., Grillner, S., Hökfelt, T., and Ottoson, D., eds) pp. 173–187, Raven Press, New York
9. Lindau, M., Hartmann, J., and Scepek, S. (1994) *Ann. N. Y. Acad. Sci.* **710,** 232–247
10. Scepek, S., and Lindau, M. (1993) *EMBO J.* **12,** 1811–1817
11. Angleson, J. K., Cochilla, A. J., Kilic, G., Nussinovitch, I., and Betz, W. J. (1999) *Nat. Neurosci.* **2,** 440–446
12. Cochilla, A. J., Angelson, J. K., and Betz, W. J. (2000) *J. Cell Biol.* **150,** 839–848
13. Lollike, K., Lindau, M., Calafat, J., and Borregaard, N. (2002) *J. Leukocyte Biol.* **71,** 973–980
14. Bokvist, K., Holmqvist, M., Gromada, J., and Rorsman, P. (2000) *Pflugers Arch.* **439,** 634–645
15. Nemoto, T., Kimura, R., Ito, K., Tachikawa, A., Miyashita, Y., Iino, M., and Kasai, H. (2001) *Nat. Cell Biol.* **3,** 253–258
16. Lindau, M., and Neher, E. (1988) *Pflügers Arch. Eur. J. Physiol.* **411,** 137–146
17. Fidler, N., and Fernandez, J. M. (1989) *Biophys. J.* **56,** 1153–1162
18. Hartmann, J., Scepek, S., and Lindau, M. (1995) *J. Physiol. (Lond.)* **483,** 201–209
19. Fernandez, J. M., Neher, E., and Gomperts, B. D. (1984) *Nature* **312,** 453–455
20. Nüsse, O., and Lindau, M. (1988) *J. Cell Biol.* **107,** 2117–2124
21. Nüsse, O., Lindau, M., Cromwell, O., Kay, A. B., and Gomperts, B. D. (1990) *J. Exp. Med.* **171,** 775–786
22. Neher, E. (1988) *J. Physiol. (Lond.)* **395,** 193–214
23. Nüsse, O., and Lindau, M. (1993) *Cell Calcium* **14,** 255–269
24. Howell, T. W., Cockcroft, S., and Gomperts, B. D. (1987) *J. Cell Biol.* **105,** 191–197
25. Yamanaka, G., Eckstein, F., and Stryer, L. (1986) *Biochemistry* **25,** 6149–6153
26. Pfeuffer, T., and Eckstein, F. (1976) *FEBS Lett.* **67,** 354–358
27. Tai, P.-C., and Spry, C. J. F. (1981) *Br. J. Hematol.* **49,** 219–226
28. Barrowman, M. M., Cockcroft, S., and Gomperts, B. D. (1986) *Nature* **319,** 504–507
29. Zimmerli, S., Majeed, M., Gustavsson, M., Stendahl, O., Sanan, D. A., and Ernst, J. D. (1996) *J. Cell Biol.* **132,** 49–61
30. Parsons, T. D., and Sterling, P. (2003) *Neuron* **37,** 379–382
31. Scepek, S., and Lindau, M. (1997) *Blood* **89,** 510–517
32. Mair, N., Haller, T., and Dietl, P. (1999) *Am. J. Physiol.* **276,** L376–382
33. Hansen, N. J., Antonin, W., and Edwardson, J. M. (1999) *J. Biol. Chem.* **274,** 22871–22876
34. Guo, Z., Turner, C., and Castle, D. (1998) *Cell* **94,** 537–548
35. Hartmann, J., Scepek, S., Hafez, I., and Lindau, M. (2003) *J. Biol. Chem.* **278,** 44920–44927

Membrane Transport, Structure, Function, and Biogenesis:

Differential Regulation of Exocytotic Fusion and Granule-Granule Fusion in Eosinophils by Ca^{2+} and GTP Analogs

Jana Hartmann, Susanne Scepek, Ismail Hafez and Manfred Lindau

J. Biol. Chem. 2003, 278:44929-44934.
doi: 10.1074/jbc.M306014200 originally published online July 9, 2003